

Frosting Experiments for a Heat Pump Having a One-Row Spine-Fin Outdoor Coil

W.A. Miller

ABSTRACT

A high-efficiency, air-to-air, split-system residential heat pump of nominal 3-ton capacity was instrumented and tested in the heating mode under laboratory conditions. The coefficient of performance (COP) and heating capacity of the system were measured during steady-state, dehumidifying, and frosting/defrosting conditions, with major emphasis placed on the dynamic frosting operation of the system. The study encompassed an evaluation of system and component performance for ambient temperature levels between 47 and 17°F (8.3 and -8.3°C) and for discrete relative humidity levels ranging from 50% to 90%.

Seasonal analyses were conducted for determination of the magnitude of frosting losses and defrosting losses for heat pumps having a one-row spine-fin outdoor heat exchanger.

INTRODUCTION

Performance data for air-source heat pumps have customarily been presented as steady-state capacity and COP tabulated for a range of outdoor dry-bulb temperatures. Estimates of COP and capacity defrosting degradations in the "frosting range" of outdoor temperatures, i.e., between 47 and 17°F (8.3 and -8.3°C), are sometimes included; however, little attention has been paid to the losses incurred while frost is accumulating on the outdoor coil, i.e., the frosting losses. Merrill (1981) conducted frosting tests on two heat pumps for development of correlations usable in seasonal performance models. The study revealed that the frost growth rate on an outdoor plate fin heat exchanger occurs in a two-step process. Frosting studies conducted by Bonne et al. (1978) on a heat pump having a spine-fin outdoor heat exchanger revealed more of a gradual increase in frost accumulation.

The results described in this paper are from the third of a series of laboratory tests (Domingorena 1978; Domingorena and Ball 1980; Miller 1980; Miller 1982) performed at Oak Ridge National Laboratory (ORNL) which were aimed at providing detailed characterization of the frosting losses as well as steady-state performance data.

EXPERIMENTAL SETUP

Heat Pump

The heat pump selected for this study had one of the highest efficiency ratings commercially available at the time the tests were conducted. The one-row spine-fin outdoor heat exchanger has two parallel refrigerant circuits. The indoor coil is of the more common tube-and-plate fin construction.

Liquid refrigerant is throttled in the heating mode by a thermostatic expansion valve and distributor tubes. The control bulb for the expansion valve is attached to the suction line of the compressor, and the external equalizer is located at the evaporator exit. This design increases the capacity of the outdoor coil by allowing a greater refrigerant flow through the heat exchanger, as compared with the conventional design, i.e., control bulb placed at the external equalizer.

The heat pump has no suction line accumulator, and the automatic defrost control is based on the evaporator inlet refrigerant temperature and an elapsed time control set to operate on a 90-min control cycle.

Test Stand

The split-system heat pump used in the experimental study was installed in two separate air loops, one loop housing the indoor unit and the other housing the outdoor unit.

Each loop was constructed of glass-fiber duct board backed by aluminum for structural strength. Sharp-edged orifice plates were installed in both test loops to measure the airflow across each unit. Thermocouple grids were used to measure the average air temperature entering and leaving each individual unit. The moisture content in the air loop containing the outdoor unit was varied by injecting steam into the loop airstream. Instrument air (dry air) was used to lower the moisture content for low-humidity test runs. Relative humidity was measured by two hygrosensors. One sensor used for humidity control was positioned at the entrance of the outdoor unit, and another sensor was placed just downstream of the outdoor unit. A centrifugal fan, driven by a variable-speed motor, was placed in series with the fan of the outdoor unit to maintain a zero static pressure drop across the outdoor unit and thus simulate free-flow conditions. Air temperature within the outdoor loop was tempered by using auxiliary heaters powered by a variable voltage transformer, and the air within the outdoor loop was cooled by the outdoor unit.

Refrigerant flow rate was measured using a turbine flowmeter. Refrigerant temperatures and pressures were measured with thermocouples and pressure transducers connected at various strategic locations in the refrigerant circuit. Electric power consumption was measured with thermal-watt converters.

Calculations of the heat pump's performance based on air-side measurements were within 3% of those based on refrigerant-side measurements.

EXPERIMENTAL PROCEDURE

Steady-State Tests

Steady-state dry coil testing commenced once the heat pump had achieved proper indoor and outdoor ambient conditions. The data acquisition system (DAS) was then enabled to monitor and record refrigerant temperatures and pressures plus power consumptions and refrigerant mass flow rates. These parameters were recorded as average values within the time span of an integral number of oscillations of refrigerant flow rate. The approximately periodic fluctuation of refrigerant flow rate was caused by an unstable "hunting" operation of the thermostatic expansion valve, which was caused by a mismatch of outdoor heat exchanger and expansion valve capacity.

With outdoor temperatures of 35 and 30°F (1.7 and -1.1°C), and relative humidities greater than 70%, frosting of the outdoor heat exchanger began before data collection could start. Thus, direct measurement of steady-state performance at these temperature and humidity levels was not possible. The steady-state performance was extrapolated from the start of each test by using the slope of the curves representing reduced test data per respective temperature and relative humidity test run.

Frosting Tests

Frosting tests were performed to observe the effect of relative humidity and temperature on heat pump COP and heating capacity. The time of frost initiation and the duration of each frosting test were detected visually and noted for each test run. The DAS was again used to monitor and record performance parameters, as was done in the steady-state tests. The airflow across the outdoor unit was also recorded and used as the criterion for defrost initiation of the heat exchanger in the outdoor unit. If the airflow was reduced by at least 50% of its nominal value [$1.32 \text{ m}^3/\text{s}$ ($2800 \text{ ft}^3/\text{min}$)] by frost buildup, the defrost cycle was manually started. (The automatic defrost control installed in this heat pump was bypassed in order to observe the effects of severe frost accumulations on the outdoor heat exchanger of this unit.)

Defrosting Test Procedure

Defrosting tests were begun at the termination of each frosting test. The time required for defrosting was noted, and instantaneous values of compressor power consumption, compressor high- and low-side pressures and temperatures, and the temperature of the refrigerant exiting the outdoor heat exchanger were monitored and recorded at 8-s intervals by the DAS. Upon completion of the defrost cycle, the heat pump was manually restored to heating-mode operation.

EXPERIMENTAL RESULTS

The heating-mode performance of a heat pump is usually characterized by the COP and the heating capacity. These quantities are affected by the outdoor heat exchanger capacity, which is, in turn, dependent on the driving potentials of ambient temperature and humidity levels. System performance was examined in terms of these driving potentials for ambient conditions that allow for a dry evaporator surface, that produce a wet surface, and, finally, that produce frosting on the coil. The results of these analyses for dry and wet coils were combined to gain an understanding of the transient operation under frosting conditions.

Steady-State System Performance Observed During Dry Outdoor Coil Operation

The COP, heating capacity, and outdoor heat exchanger capacity increased linearly with increasing ambient temperature under dry coil conditions, as characterized in figure 1. The system COP (figure 1) increased from 2.12 at 17°F (-8.3°C) to 2.9 at (47°F) (8.3°C); the heating capacity increased from 18,800 Btu/h (5.51 kW) at 17°F (-8.3°C) to 31,190 Btu/h (9.14 kW) at 47°F (8.3°C).

The compressor efficiency* improved from 46% at 17°F (-8.3°C) to 53.5% at 47°F (8.3°C).

COP and Heating Capacity Observed for a Wet Outdoor Heat Exchanger

System COP and capacity improved slightly under conditions of high humidity in the nonfrosting range. With a 47°F (8.3°C) ambient air temperature and a relative humidity of 60% or greater, the outdoor coil surface temperature is below the dew point of the air but above the freezing point of water. Thus the coil is wet but not frosted. As shown in figure 2, the average COP at this temperature was observed to increase from 2.9 to 2.95 and 3.05 as the relative humidity was increased by increments of 10 percentage points from 60% to 80%. The corresponding heating capacities were 31,200, 32,900, and 34,200 Btu/h (9.14, 9.64, and 10.0 kW).

The improvements in COP and heating capacity mentioned above are the result of an increased outdoor heat exchanger capacity. For a constant dry-bulb temperature, an increase in the relative humidity yields higher rates of mass transfer and an increased latent heat contribution to the capacity of the outdoor heat exchanger.

*Compressor efficiency is defined here as the ratio of isentropic compressor output (measured across the shell) to the measured power input.

Test results at 40°F (4.4°C) for relative humidities greater than 70% revealed an initial improvement in system performance that was observed with the outdoor coil surface wet rather than frosted. The COP (figure 3) increased from 2.75 (base case performance) to values of 2.82, 2.85, and 2.92 as the respective relative humidity was increased from 70% to 90%. Similarly, the heating capacity increased from 27,750 Btu/h (8.1 kW) to values of 29,200, 30,400, and 31,500 Btu/h (8.5, 8.9, and 9.23 kW) as the relative humidity was increased from 70% to 90%. The increase in system performance is due to the increased mass transfer rate as the moisture content of the air is enhanced above moisture levels present at 60% humidity. The augmented mass transfer increased the evaporator tube wall temperature, as seen in figure 4. This increase in the tube wall temperature over the two-phase region of the outdoor heat exchanger resulted in a delay in the onset of frosting as the relative humidity was increased. Frosting was visually observed 35 min into the 70% test run; at 80% and 90% relative humidities, frosting did not begin until 85 and 160 min, respectively, of run time had elapsed.

At the onset of the 80% and 90% test runs conducted at 40°F (4.4°C), the outdoor coil was initially saturated with water, and a flow of condensate from the coil was observed until frosting began. The accumulation of water on the outdoor heat exchanger gradually increased the resistance to heat flow and thus lowered the tube wall temperature to a point favorable for frost formation, as seen in figure 4. Once frosting began, the higher relative humidities, reflecting an increase in the moisture content of the air, enhanced the rate of frost accumulation, resulting in greater rates of performance degradation. The increase in slope for relative humidities greater than 70% in figure 3 graphically depicts the above observation.

The trends in system performance present at 40°F (4.4°C) were not observed at ambient temperatures less than 40°F (4.4°C). For tests conducted at ambient temperatures of 35, 30, 20, and 17°F (1.7, -1.1, -6.7, and -8.3°C), increasing the relative humidity increased the rate of frost accumulation on the outdoor heat exchanger. However, frost accumulation did not occur in distinct phases, as observed by Merrill (1981). The threshold of frosting was visually observed at 60% relative humidity for the 35 and 30°F (1.7 and -1.1°C) ambient conditions, but at the lower ambient temperatures of 20 and 17°F (-6.7 and -8.3°C) the threshold of frosting was visually observed to occur at 70% relative humidity.

At an ambient temperature of 35°F (1.7°C), a temperature favorable to frosting, the system COP and heating capacity decreased for relative humidity levels greater than 60% (see figures 5 and 6). The increased moisture content in the air increased the rate of performance degradation because of the increased frosting rates on the outdoor heat exchanger.

The COP at 70% relative humidity decreased from an initial value of 2.58 to 2.18, a 15% reduction within 80 min of operation. At the higher humidity of 80%, the COP decreased from 2.63 to 2.15, an 18% reduction within 60 min of operation.† The COP degraded by 18% of steady-state value within 50 min of heat pump operation for the 90% relative humidity test conducted at 35°F (1.7°C). The heating capacity observed during the 70%, 80%, and 90% relative humidity tests decreased by 24% of the initial values; however, the time required for the 24% degradation decreased from 100 to 55 and 45 min respectively (figure 6).

Frosting was light during the 60% relative humidity test conducted at 30°F (-1.1°C), and no noticeable reduction in system performance was observed (figures 7 and 8). Incrementing the relative humidity to 70% produced a noticeable frost accumulation on the outdoor heat exchanger; however, it was only moderately frosted at the termination of the experiment. The COP during the 70% humidity test decreased from an initial value of 2.45 to 2.15 within 160 min of operation, while the corresponding heating capacity dropped from 23,650 to 19,500 Btu/h (6.93 to 5.71 kW). The increase of relative humidity above 70% augmented the rate of frost accumulation on the outdoor heat exchanger to a point at which roughly 90% of the coil was blocked with frost within 50 min of operation. The COP dropped from approximately 2.5 to values of 2.1 and 2.0, respectively, for the 80% and 90% humidity

†All frosting tests were terminated once the outdoor airflow was reduced by 50% of its nominal value [1.32 m³/s (2800 ft³/min)].

tests (figure 7). The heating capacity dropped from nominally 25,000 Btu/h (7.3 kW) to values of 19,250 Btu/h (5.4 kW) and 18,000 Btu/h (5.27 kW), respectively, for the 80% and 90% humidity tests (figure 8).

No new trends in system performance were observed for tests conducted at 20°F (-6.7°C) and at 17°F (-8.3°C). Results for these tests are discussed by Miller (1980 and 1982) but are omitted here because of similarity of results.

Effect of Frost on Evaporator Tube Wall Temperature

The frost accumulation on the outdoor heat exchanger increased the resistance to heat flow and thus reduced both evaporator tube wall temperature and refrigerant suction pressure at the inlet to the compressor. Using the 30°F (-1.1°C) test runs as typical results, the tube wall temperature, characterized in figure 9, was nominally 22°F (-5.55°C) for the low-humidity test runs of 50% and 60%. The spine fins, having an average temperature below 32°F (0°C), immediately began to frost for the 30°F (-1.1°C) test having humidity levels of 70% and greater. The wall temperature decreased from 20°F (-6.7°C) to 6°F (-14°C) within 50 min during the 90% relative humidity test (figure 9). The suction pressure at the inlet to the compressor shows nearly identical trends to those of the tube wall temperature because the saturation temperature in the two-phase region of the outdoor heat exchanger directly affects refrigerant pressure to the compressor.

Compressor Performance During Frosting Conditions

The reduction of suction pressure yielded corresponding reductions in compressor inlet refrigerant density, which, in turn, yielded corresponding reductions in both refrigerant mass flow rate and compressor power consumption. Again using typical results observed at 30°F (-1.1°C), the reduction of refrigerant density, characterized in figure 10, caused the refrigerant mass flow rate to decrease from 260 lb_m/h (118 kg/h) to approximately 190 lb_m/h (86.4 kg/h) for the 90% relative humidity test. The corresponding power consumption decreased from 2250 W to approximately 1950 W. The 26% reduction in mass flow rate as compared to the 15% reduction in compressor power lowered the overall efficiency of the compressor and motor. The motor-compressor efficiency for the 90% humidity condition dropped from 51.5% to 46% within 30 min of operating time.

TRANSIENT OPERATION DURING DEFROSTING CYCLE

Defrosting of the outdoor heat exchanger produced transients in refrigerant circuit temperatures and pressures and compressor power consumption. The results of a typical defrosting test, following the 30°F (-1.1°C), 70% relative humidity frosting test, are presented in figure 11 for observation of defrosting phenomena.

Energizing the four-way reversing valve at the start of the defrosting operation results in an initial drop in head pressure and an initial jump in suction pressure because of the switching of refrigerant lines within the reversing valve. Within 32 s, the discharge pressure dropped from 188.5 to 117 psia (1.3 to 0.81 MPa), and the suction pressure increased from 45.6 to 104.7 psia (314 to 721 kPa). After these initial perturbations, both suction and head pressure decreased for a period of 50 s. Within this period, the refrigerant accumulated in the outdoor heat exchanger, and the indoor heat exchanger became nearly evacuated of refrigerant. The head pressure then started to increase, allowing throttling through the expansion valve to begin. After 80 s of defrosting, there was a steady increase in suction pressure, head pressure, and also compressor power. This increase persisted until manual termination of the defrosting cycle, which, under automatic operation, would occur after the refrigerant temperature leaving the outdoor heat exchanger reached 55°F (12.7°C). At termination of the defrosting cycle, the compressor power and high- and low-side pressures again followed trends observed at the start of the cycle. However, it was inferred from temperature and pressure data that a two-phase mixture of refrigerant was entering the compressor housing immediately following the

defrosting cycle. The amount of liquid entering the compressor could not be determined and is assumed to be small because of the short interval over which it was observed.

FROSTING AND DEFROSTING LOSSES

Cycling and defrosting losses are usually considered the major deterrents to efficient heat pump operation. However, few heat pump studies have investigated the losses incurred while frost is forming on the outdoor heat exchanger. These frosting losses yielded significant cumulative reductions in both COP and heating capacity for tests conducted at 1.7 and -1.1°C (35 and 30°F) having relative humidities greater than 70%.

The frosting and defrosting losses were insignificant for all ambient conditions where relative humidities were less than 60%. The frosting losses, however, did increase significantly for ambient temperatures less than 40°F (4.4°C) that had relative humidities of 70% and greater (see table 1). Frosting losses of approximately 10% were observed in COP for tests conducted at 35°F (1.7°C) and 30°F (-1.1°C) having relative humidities greater than 70%. Heating capacity degradation due to frosting for the above tests was approximately 15%. The observed nominal 10% reduction of COP and 15% reduction of heating capacity for the above 80% and 90% humidity tests occurred within 60 min, at a point in time when the outdoor heat exchanger was nearly blocked with frost. Similar results were also observed for tests conducted at 20°F (-6.7°C) when relative humidities were greater than 80%. With the outdoor coil nearly blocked with frost, a 10% loss in COP and a 15% loss in cumulative heat output was observed within 75 min of operation due to frost accumulation on the outdoor heat exchanger.

The capacity losses due to frosting were larger than the capacity losses due to chilling of the indoor airstream during defrosting. Frosting of the outdoor heat exchanger produced about a 15% degradation[‡] in heating capacity for tests conducted at 30 and 35°F (-1.1 and 1.7°C) with relative humidities of 80% and 90%. Chilling of the indoor airstream during defrosting further degraded the capacity output by approximately 8% for tests conducted at 30 and 35°F (-1.1 and 1.7°C) having relative humidities of 80% and 90%.

Defrosting degradation of COP was slightly larger than that of heating capacity because auxiliary heat was used to temper the chilled indoor airstream. The additional power consumption, 5-kW auxiliary heat, caused higher COP degradation than capacity degradation for all tests listed in table 1.

ADEQUACY OF DEFROSTING CONTROLS

The time-and-temperature defrosting control is used by the majority of heat pump manufacturers. A timing cam can be set to operate on a 30-, 45-, or 90-min cycle and will initiate a defrosting cycle within a 10-min period prior to completion of the cycle provided the refrigerant temperature at the inlet to the evaporator is less than 28°F (-2.2°C) for the particular unit tested.

Experimental results show that the 90-min cycle allows defrosting operations too infrequently for ambient conditions less than 40°F (4.4°C) having relative humidities greater than 70%. The outdoor heat exchanger was observed to be nearly blocked by frost within 50 min of frosting operation for relative humidities greater than 70% and ambient temperatures between 30 and 35°F (-1.1 and 1.7°C). Reducing the period of the cycle would alleviate severe frost buildups, but shorter cycles would increase the number of needless, or false, defrost operations that would occur at low humidities. An unnecessary defrosting operation at 30°F (-1.1°C) yielded a 3% reduction of steady-state COP and a 1.3% reduction in heating capacity. Although these losses are minimal, repetitive defrosting operations could possibly be more detrimental to overall seasonal performance than severe frosting of the outdoor heat exchanger. Either situation could increase wear on the compressor.

[‡]Degradations in COP and heating capacity, as caused by frosting, were calculated using, as a base, COP and heating capacity values that were extrapolated to the beginning of each frosting test.

A demand defrosting device sensing the temperature difference between ambient air and the evaporator tube wall or refrigerant would eliminate needless defrosting operations. The demand sensor, currently available on the open market, would also control heavy frost accumulations on the outdoor heat exchanger better than the time-and-temperature defrosting sensor does. A comparative analysis of frosting losses, listed in table 2, was made using experimental data and simulating both demand defrosting logic and time-and-temperature defrosting logic. The demand defrosting logic was based on an experimentally observed 15 F° (8.3 C°) temperature difference between ambient air and evaporator tube wall temperature as being appropriate for defrost initiation, and the time-and-temperature logic was based on a 90-min cycle with previously mentioned temperature initiation and termination points.

A comparison of these defrosting schemes reveals that frosting losses are nominally 30% less for the demand scheme than for the time-and-temperature scheme, as seen in table 2. Seasonal performance studies (SAI 1980) substantiate the above results. The seasonal analysis study evaluated heat pump seasonal performance using eight different defrosting control strategies as applied to frosting test data observed on a high-efficiency air-to-air heat pump. The seasonal performance results revealed the demand defrosting scheme to be the superior defrosting logic, in regard to minimizing energy consumption, as compared to time-and-temperature defrosting logics.

SEASONAL ANALYSIS OF FROSTING AND DEFROSTING

The heat pump selected for this study was observed to be susceptible to frosting degradations in COP and heating capacity for outdoor ambient temperatures between 40 and 17°F (4.4 and -8.3°C) having relative humidities greater than 70%. However, yearly analysis of heat pump performance is required for determining the magnitude and significance of frosting losses.

Seasonal analyses were conducted using frosting loss coefficients (Miller 1980, Sect. 8.3) that express the percentage loss in cumulative steady-state heat output and COP. These frosting loss coefficients were derived from experimental data and are functions of outdoor ambient temperature and humidity and heat pump operating time. The frosting loss coefficients were coupled to a quadratic interpolation routine** and incorporated in a seasonal performance computer code developed by Rice, Emerson, and Fischer (to be published). Defrosting calculations were based on field data measurements collected by Baxter (to be published) for a heat pump identical to the model heat pump tested in the laboratory. Baxter (to be published) supplied average heating season values for length of defrost period (4.9 min), average chilling rate of indoor airstream (5.2 kW), and average defrosting power consumption rate (11.2 kW) as measured during the 1981-1983 field tests.††

Seasonal analysis for the University of Tennessee ACES house, located in Knoxville, TN, revealed a 4.29% increase in heating seasonal energy consumption due to frosting of the outdoor heat exchanger. The heating seasonal COP was degraded by 4.3% because of frosting; however, the COP was further degraded by 11.8% because of defrosting of the outdoor coil. These calculations are in excellent agreement with measured field test losses observed by Baxter (to be published). Baxter observed a 3.5% loss in heating seasonal COP due to frosting, and an 11.2% loss in heating seasonal COP due to defrosting.

Further seasonal analysis for the ACES house using Engineering Weather Data (Departments of the Air Force, the Army, and the Navy 1978) for Chicago, IL, was made for observation of frosting losses under winter weather conditions more severe than those for Knoxville, TN. Heating seasonal COP was degraded by 4.36% by frosting of the outdoor heat exchanger. Defrosting of the outdoor heat exchanger further degraded seasonal heating COP by 11.1%.

**Given the ambient dry-bulb temperature and relative humidity, the moist air enthalpy was calculated and used as the interpolating variable for calculation of frosting loss coefficients.

††Heat pump time and temperature defrost sensor set to 90-min timed interval defrost control for duration of field test.

Seasonal analysis clearly shows frosting/defrosting degradation to be due primarily to defrosting of the outdoor heat exchanger. However, the more susceptible the outdoor heat exchanger is to frost accumulations, the greater will be the penalty in increased power consumption and COP degradation due to defrosting. Results indicate that demand- or time-controlled defrost intervals could possibly be extended at the expense of greater frosting losses in order to lower seasonal losses due to frosting/defrosting, provided system reliability would not be compromised.

CONCLUSIONS

1. Frosting and defrosting losses were insignificant for all laboratory tests conducted with outdoor relative humidities of 60% or less.
2. Seasonal performance analysis incorporating the derived frosting loss coefficients (Miller 1982) revealed frosting losses in heating seasonal COP to be approximately 4% for both Knoxville, TN (DOE Region 4), and Chicago, IL (DOE Region 5).
3. Defrosting of the one-row spine-fin outdoor heat exchanger yielded heating seasonal COP degradations roughly three times the magnitude of frosting losses for seasonal analyses conducted for both Knoxville, TN (DOE Region 4), and Chicago, IL (DOE Region 5).
4. The use of auxiliary heat during defrosting periods caused significant cumulative reductions in COP. Defrost power consumption yielded nominally 15% degradations of COP for lab tests conducted at 30 and 35°F (-1.1 and 1.7°C) and at relative humidities greater than 70%.
5. For nonfrosting dehumidifying conditions at 47°F (8.3°C), the COP improved 5% and the heating capacity improved 10% by increasing the outdoor relative humidity from 60% to 80%.
6. The heat pump COP and capacity, measured at 40°F (4.4°C) as a function of time after system start-up, decreased with time because of frost accumulation on the outdoor heat exchanger. However, the heat pump COP and capacity initially improved, nominally 5% and 10% respectively, by increasing the ambient relative humidity from 50% to 90%.
7. The onset of frosting on the outdoor heat exchanger was delayed 125 min by increasing the relative humidity from 70% to 90% for the 40°F (4.4°C) tests. The increase in mass transfer, due to higher moisture content of the air, yielded greater latent heat contributions to the evaporator. The augmented heat gains caused an increase in evaporator tube wall temperature, thus delaying the onset of frosting, as compared to the 70% relative humidity test run.

REFERENCES

- Baxter, V. D.; and Moyers, J. C. To be published. "Air source heat pump: field measurement of cycling, frosting, and defrosting losses, 1981-1983."
- Bonne, U.; Jacobson, R. D.; Patani, A.; and Aagard, R. L. 1978. "Seasonal efficiency of residential combustion and heat pump systems." International Symposium on Simulation Modeling and Decision in Energy Systems, Montreal, June.
- Departments of the Air Force, the Army, and the Navy. 1978. "Engineering weather data." AFM88-29, TM5-785, NAVFAC P-89, July 1.
- Domingorena, A. A. 1978. "Performance evaluation of a low-first-cost, three-ton, air-to-air heat pump in the heating mode." ORNL/CON-18, Oak Ridge, TN: Oak Ridge National Laboratory, October.
- Domingorena, A. A.; and Ball, S. J. 1980. "Performance evaluation of a selected three-ton, air-to-air heat pump in the heating mode." ORNL/CON-34, Oak Ridge, TN: Oak Ridge National Laboratory, January.
- Merrill, P. 1981. "Heat pumps 'on-off' capacity control and defrost performance using demand and time-temperature defrost controls." *ASHRAE Trans.* 87, Part 1, pp. 381-393.

- Miller, W. A. 1980. "The influence of ambient temperature and relative humidity on the heating mode performance of a high-efficiency air-to-air heat pump." M.S. thesis, Department of Mechanical Engineering, University of Tennessee, Knoxville.
- Miller, W. A. 1982. "Laboratory evaluation of the heating capacity and efficiency of a high-efficiency, air-to-air heat pump with emphasis on frosting/defrosting operation." ORNL/CON-69, Oak Ridge, TN: Oak Ridge National Laboratory, December.
- Rice, C. K.; Emerson, C. J.; and Fischer, S. K. To be published. "The Oak Ridge heat pump models: II. An annual performance factor/loads model for residential heat pumps."
- SAI. 1980. "Variable interval time/temperature defrost control system evaluation." SAI-444-80-472-LJ (rev.), Science Applications, Inc., Oct. 1.

ACKNOWLEDGMENTS

This research was sponsored by the U.S. Department of Energy under contract W-7405-eng-26 with the Union Carbide Corporation.

TABLE 1
Loss in Performance due to Frosting/Defrosting

Relative humidity (%)	Steady-state performance		Performance under frosting conditions					
	COP	QH (Btu/h)	COP		ΔCOP^a , %		ΔQH^a , %	
			Fr ^b	Fr/def ^c	Fr	Def ^d	Fr	Def
Temperature = 4.4°C (40°F)								
60	2.74	28,507	2.67	2.61	2.21	2.49	3.58	1.16
70	2.82	29,200	2.62	2.36	7.23	9.03	11.02	4.11
80	2.87	30,800	2.73	2.35	4.82	13.36	7.66	6.38
90	2.89	31,168	2.79	2.47	3.31	11.07	5.95	5.04
Temperature = 1.7°C (35°F)								
60	2.64	26,637	2.58	2.51	2.45	2.77	4.17	1.32
70	2.73	27,740	2.45	2.28	10.18	6.24	15.18	2.58
80	2.76	28,977	2.46	2.04	10.87	15.43	16.30	7.77
90	2.61	27,782	2.40	1.87	8.28	20.47	13.90	11.08
Temperature = -1.1°C (30°F)								
70	2.54	23,800	2.35	2.24	7.50	4.33	6.33	2.00
80	2.75	27,502	2.43	2.00	11.73	15.41	15.52	8.06
90	2.63	26,138	2.32	1.87	11.88	17.20	16.76	9.15
Temperature = -6.7°C (20°F)								
80	2.22	20,954	2.19	1.98	1.46	9.16	5.76	4.16
90	2.33	21,672	2.10	1.79	9.58	13.13	14.08	6.61

^a ΔCOP , ΔQH —Percentage breakdown of frosting and defrosting based on steady-state COP and QH as determined from each temperature and relative humidity test run.

^bFr—Performance measured over duration of respective test, not including defrosting operation.

^cFr/def—Performance measured over duration of respective test, including defrosting operation.

^dDef—Performance during defrosting period including chilling of indoor air, 5-kW auxiliary heat, and defrosting power used by compressor and indoor fan.

TABLE 2
Frosting Losses Incurred as a Function of Defrosting Sensor Scheme

Ambient temperature [°C (°F)]	Relative humidity (%)	Loss (%) in average COP		Loss (%) in cumulative heat output		Elapsed time (min) prior to defrosting	
		Demand	Time and temperature	Demand	Time and temperature	Demand	Time and temperature ^a
1.67 (35)	70	1.89	4.66	4.13	7.80	~55	80
1.67 (35)	80	7.48	10.87	11.15	16.30	44	Blocked ^b
1.67 (35)	90	5.06	8.28	8.16	13.90	32	Blocked
-1.11 (30) ^c	70	5.43	4.32	2.93	0.81	~118	80
-1.11 (30)	80	9.32	11.73	12.23	15.52	42	Blocked
-1.11 (30)	90	7.06	11.88	9.53	16.76	30	Blocked

^a90-min cycle.

^bApproximately 90% of the outdoor coil was visibly observed blocked with frost; however, air was able to pass over the top of the coil.

^cCoil only partially frosted after 80 min of operation. Defrost not required.

By acceptance of this article, the publisher or recipient acknowledges the U.S. Government's right to retain a nonexclusive, royalty-free license in and to any copyright covering the article.

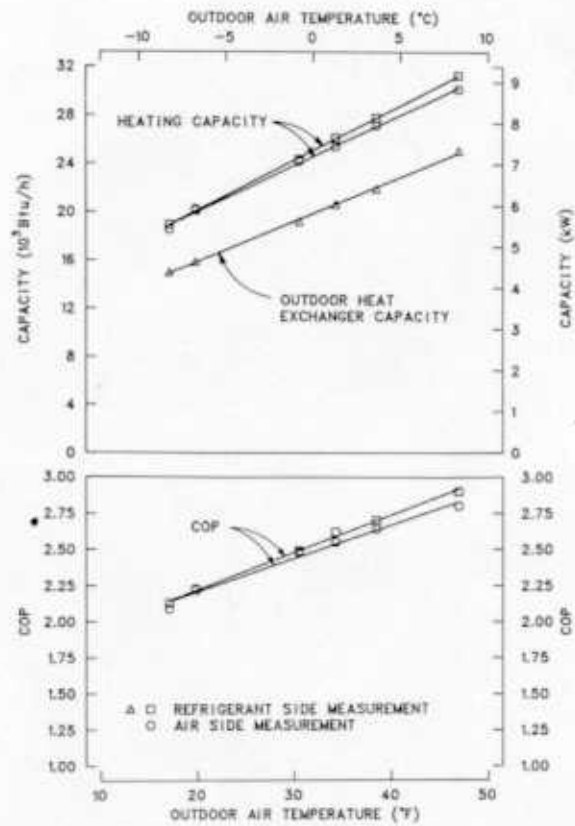


Figure 1. Steady-state system performance observed with a dry outdoor heat exchanger

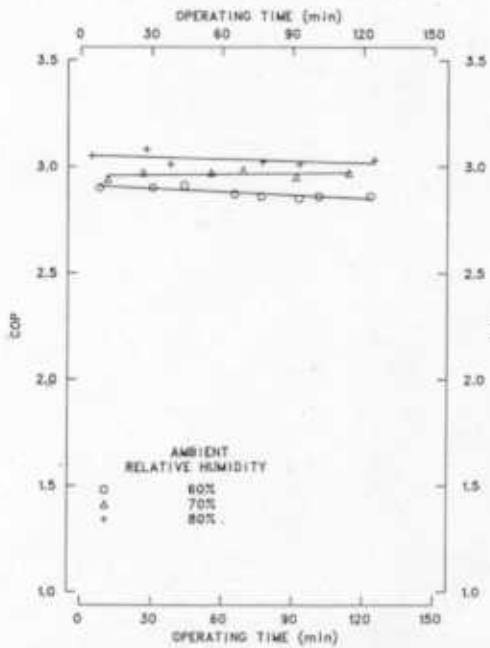


Figure 2. COP for a wet outdoor heat exchanger at an ambient temperature of 47°F (8.3°C)

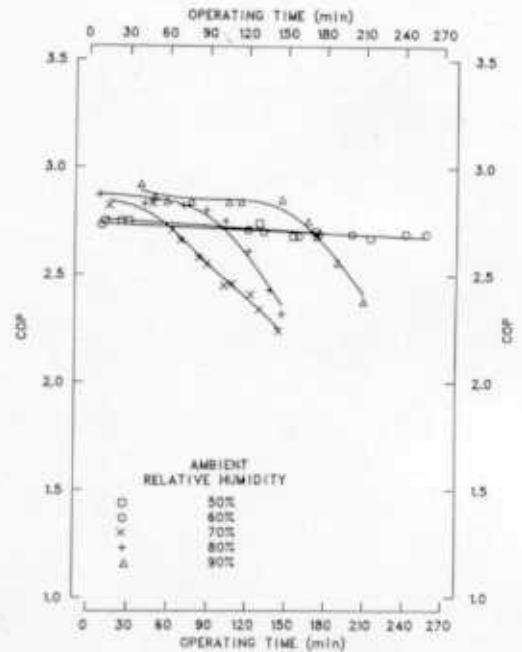


Figure 3. COP measured at 40°F (4.4°C)

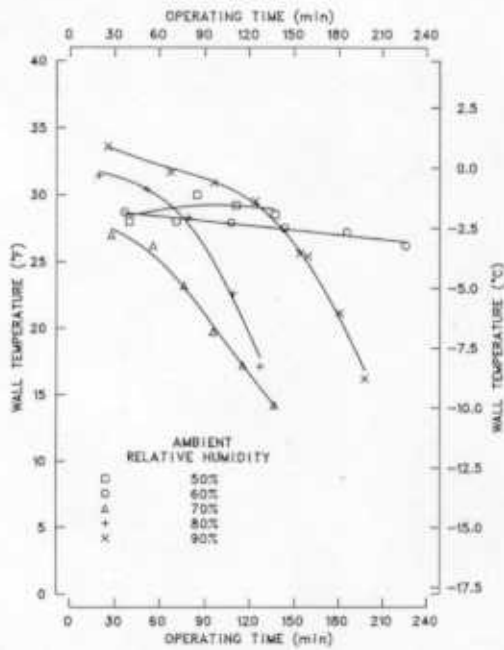


Figure 4. Average tube wall temperature over the entire two-phase region of the outdoor heat exchanger

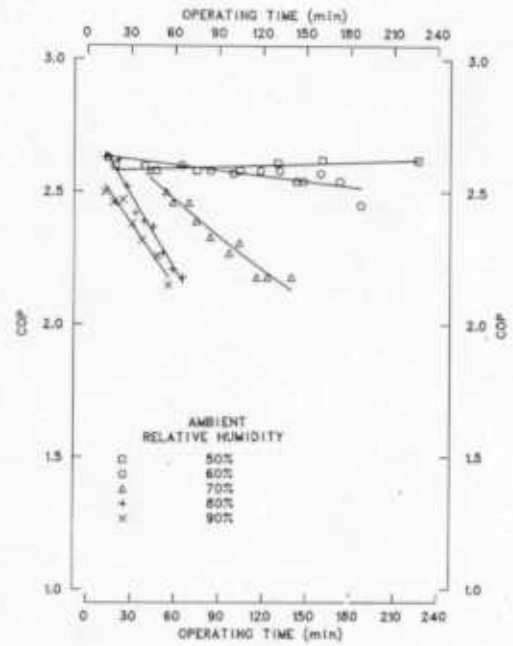


Figure 5. COP measured at 35°F (1.7°C)

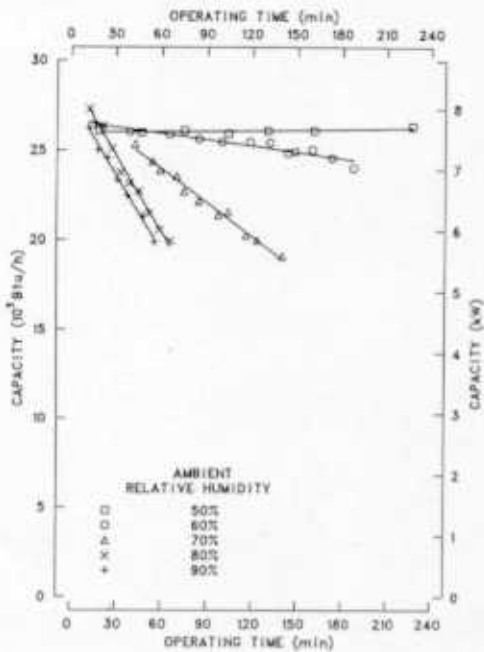


Figure 6. Heating capacity measured at 35°F (1.7°C)

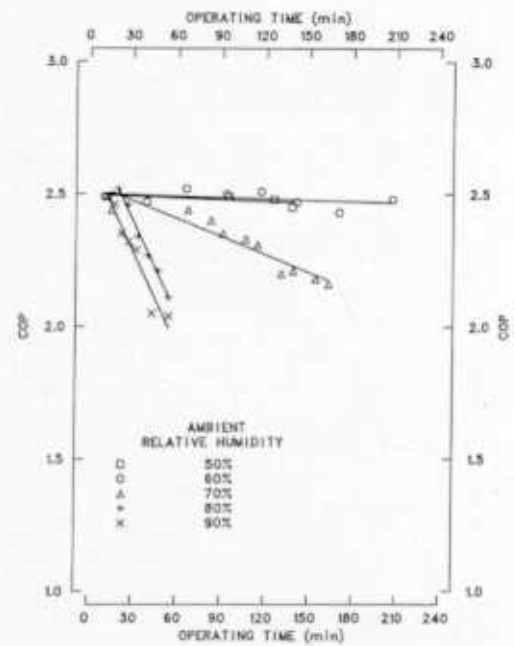


Figure 7. COP measured at 30°F (-1.1°C)

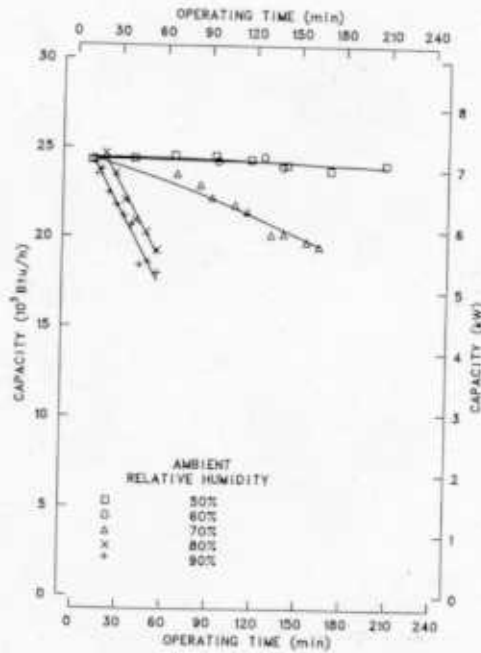


Figure 8. Heating capacity measured at 30°F (-1.1°C)

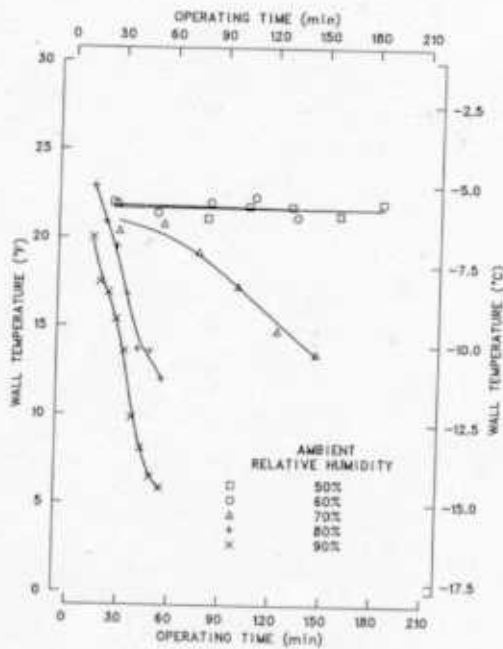


Figure 9. Average evaporator tube wall temperature observed for a 30°F (-1.1°C) ambient.

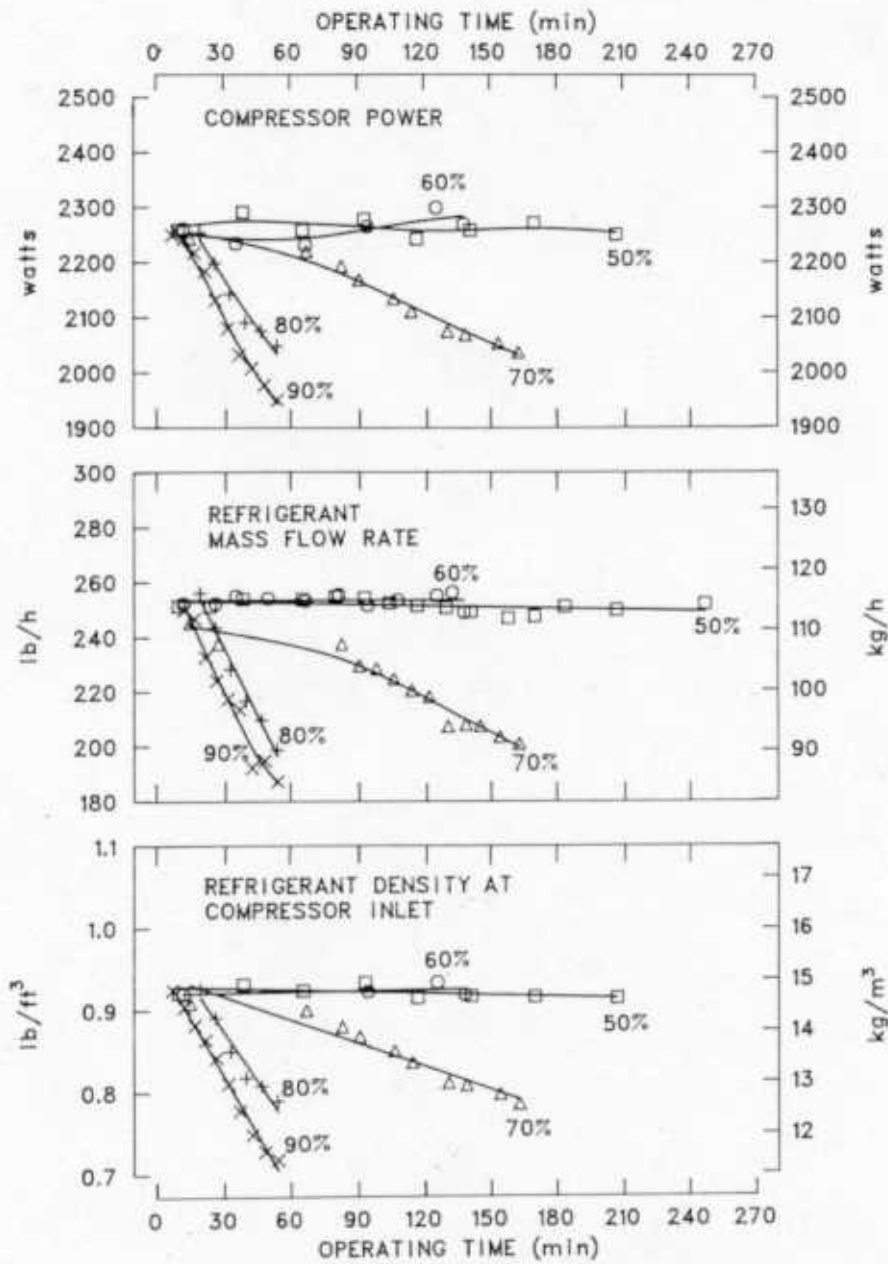


Figure 10. Performance trends observed for a 30°F (-1.1°C) ambient

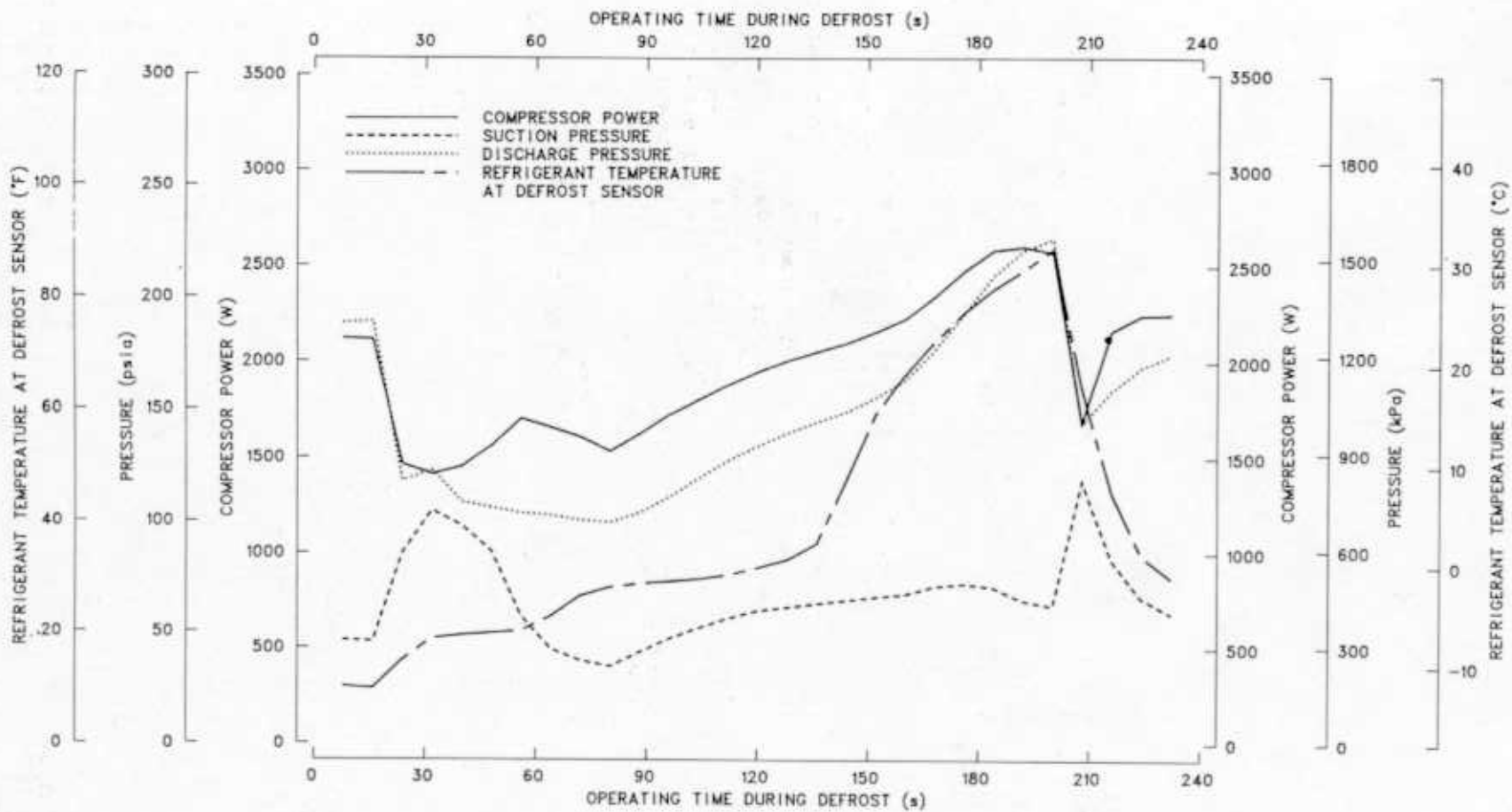


Figure 11. Defrost cycle observed following a 30°F (-1.1°C), 70% relative humidity test

DISCUSSION

J.M. Calm, Elec. Power Research Inst., Palo Alto, CA: Would you comment on seasonal performance degradation attributable to defrost disaggregated between actual defrost and concurrent supplemental heating requirements?

Does this imply an opportunity for HSPE improvement by alternative means of supplemental heating for the function such as very short duration (ie, defrost interval) thermal storage approaches?

Miller: Seasonal analyses were conducted using frosting loss coefficients derived from laboratory data on a heat pump having a one row spine fin outdoor coil. The analysis as applied to the University of Tennessee ACES house located in Knoxville, revealed defrosting to increase heating seasonal energy consumption by 15.3%. Of this energy use, that used for reverse cycle defrosting resulted in a 7.77% increase in energy consumption while the concurrent defrost tempering further increased energy consumption by 7.55%, see accompanying table. Tempering heat during defrosting comprised 49% of the increase in energy consumption due to heat pump defrosting. Results show that reducing the size of defrost tempering heater from nominal 9-KW to 5-KW; or, an alternative means of supplemental heating could improve heating seasonal performance efficiency (HSPE).

Heat Pump Dynamic Operation	Increase in Energy Consumption*	
	Heating Season, %	Annual, %
Defrost:		
Reverse Cycle	7.77	4.90
Tempering Heat	7.55	4.56
Frosting	4.50	2.87
Frost/Defrost	19.82	12.33

*Heating season energy (4669.8KWH)

Yearly season energy (7366.9KWH).

Calculations based on above consumptions and include cycling losses.

D.J. Young, Ontario Hydro, Toronto, Ont., Canada: How would you expect the frosting/defrosting losses and the annual energy increases that you described to change if a conventional plate fin-on-tube heat exchanger were used for the outdoor coil?

Miller: An abbreviated series of frosting, defrosting tests were conducted on a heat pump configured with a tube and plate fin outdoor coil, having 13 fins per inch. Results, for tests conducted at 35 F (1.7 C) outdoor temperature, revealed the unit with a tube and plate fin outdoor coil to be less susceptible to frosting losses as compared to the unit with a spine fin outdoor coil. Both spine fin and tube and plate fin coils operated under the same load as inferred from evaporator refrigerant temperatures. However, outdoor fan characteristics were probably different for both units. An accurate comparison needs to be conducted in which all other parameters can be held constant for evaluation of heat exchanger geometries.